chem2Dmat
AUGUST 31 - September 03, 2021 • ONLINE

MXENES AGAINST SARS-COV-2

Laura Fusco[a,b], Mehmet Altay Unal[c], Fatma Bayrakdar[d], Omur Besbinar[c,e], Christopher E. Shuck[f], Süleyman Yalcin[d], Mine Turktas Erken[g], Aykut Ozkul[h,s], Cansu Gurcan[c,e], Oguzhan Panatli[e], Gokce Yagmur Summak[c], Cemile Gokce[e], Marco Orecchioni[i], Arianna Gazzi[a,j], Flavia Vitale[k], Julia Somers[l], Emek Demir[l], Serap Suzuk Yildiz[d], Hasan Nazir[m], Jean-Charles Grivel[n], Davide Bedognetti[b,o,p], Andrea Crisanti[q], Kamil Can Akcali[c,r], Yury Gogotsi[f], Açelya Yilmazer[c,e], Lucia Gemma Delogu[a]

[a] Dept. of Biomedical Sciences, University of Padua, Padua, Italy; [b] Cancer Research Department, Sidra Medicine, Doha, Qatar; [c] Stem Cell Institute, Ankara University, Balgat, Ankara, Turkey; [d] Ministry of Health General Directorate of Public Health, Microbiology References Laboratory, Ankara, Turkey; [e] Dept. of Biomedical Engineering, Ankara University, Golbasi, Ankara, Turkey; [f] A.J. Drexel Nanomaterials Institute and Dept. of Materials Science and Engineering, Drexel University, Philadelphia, PA, USA; [g] Dept. of Biology, Gazi University, Ankara, Turkey; [h] Dept. of Virology, Faculty of Veterinary Medicine, Ankara University, Ankara, Turkey; [i] La Jolla Institute for Immunology, La Jolla, CA, USA; [j] Dept. of Chemical and Pharmaceutical Sciences, University of Trieste, Trieste, Italy; [k] Dept. of Neurology, Bioengineering, Physical Medicine & Rehabilitation, Center for Neuroengineering and Therapeutics, University of Pennsylvania, Philadelphia, PA, USA; [l] Oregon Health & Sciences University, Dept. of Molecular and Medical Genetics, Portland, OR, USA; [m] Dept. of Chemistry, Ankara University, Tandogan, Ankara, Turkey; [n] Deep Phenotyping Core, Sidra Medicine, Doha, Qatar; [o] Dept. of Internal Medicine and Medical Specialties (DiMI), University of Genoa, Genoa, Italy; [p] College of Health and Life Sciences, Hamad Bin Khalifa University, Doha, Qatar; [q] Dept. of Molecular Medicine, Padua University Hospital, Padua, Italy; [r] Dept. of Biophysics, Faculty of Medicine, Ankara University, Ankara, Turkey; [s] Biotechnology Institute, Ankara University, Ankara, Turkey.

INTRODUCTION

Two-dimensional transition metal carbides/carbonitrides (MXenes)[1,2] are rapidly growing as multimodal nanoplatforms in biomedicine, including against infectious diseases.[3] Here, taking SARS-CoV-2 as a model, we explored the antiviral and immunomodulatory properties of four MXenes - $Ti_3C_2T_x$, $Ta_4C_3T_x$, $Mo_2Ti_2C_3T_x$, and $Nb_4C_3T_x$. Following material synthesis and characterization, we performed detailed antiviral and deep-immune profiling experimentation (Fig. 1). We first delineated the antiviral activity of the four different highly stable MXenes. We selected four viral genotypes from the viral repository of the Microbiology References Laboratory in Turkey. We then assessed the viral inhibition by quantification of viral copy numbers and viability of Vero E6 cells. Based on this, we performed *in silico* molecular docking and proteomic analysis to reveal the mechanism of viral inhibition. Finally, because each immune subpopulation can play a different role with possible reactions to MXene-based clinical nanomedicine, we performed viability and activation assay by flow cytometry as well as a wide analysis on the production of cytokines and chemokines by Luminex. An in-depth analysis at the single-cell level towards 17 primary human immune cell subpopulations was then performed by single-cell mass cytometry looking at the impact on viability and their functionality by cytokine production.

RESULTS

Fig. 2 - Material characterization

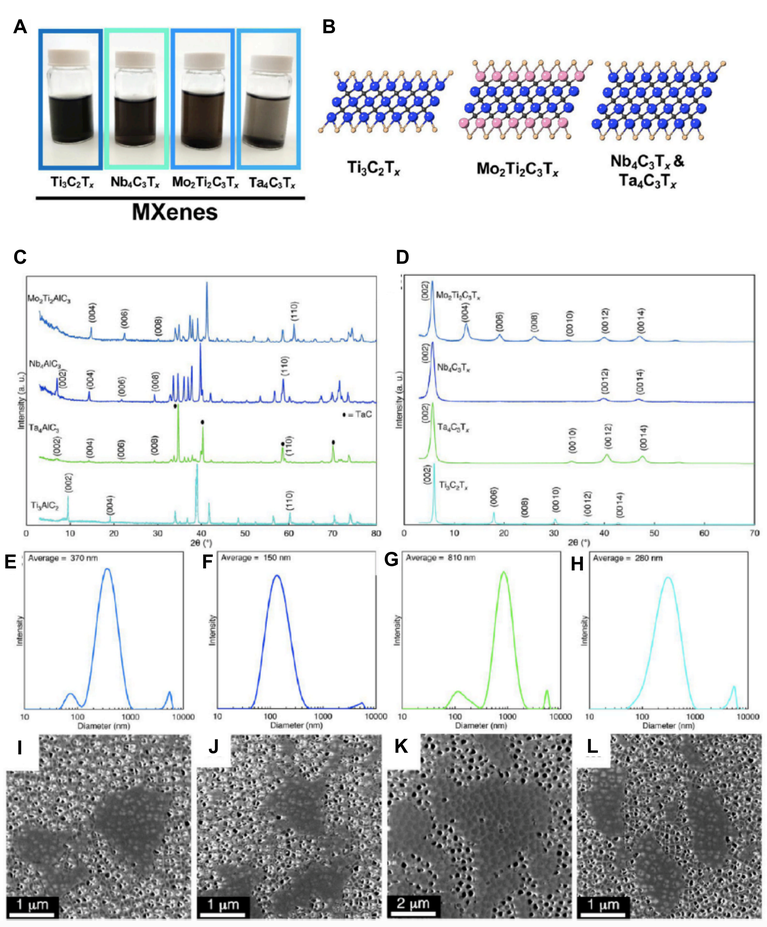

MXenes (Fig. 2A, B) were produced by selectively etching Al from MAX phases. X-ray diffraction patterns (XDR) of the precursor MAX powders (Ti_3AlC_2, Nb_4AlC_3, $Mo_2Ti_2AlC_3$, and Ta_4AlC_3) and delaminated MXenes ($Ti_3C_2T_x$, $Nb_4C_3T_x$, $Mo_2Ti_2C_3T_x$, and $Ta_4C_3T_x$) are shown in Fig. 2C, D respectively. The MAX phases have p63/mmc space group, with the (00l) and (110) peaks labeled. For Ti_3AlC_2, the (002) peak is located at 9.54° (9.26 Å), and after etching and delamination with tetramethylammonium hydroxidE, the peak shifts to 5.94° (14.78 Å) for $Ti_3C_2T_x$. Similar trends are observed for the other MAX to MXene conversions, indicating successful removal of the Al layers for all MXenes. In the MXene XRD patterns, only the (00l) peaks remain, indicating successful etching and delamination, with no impurities remaining in the MXene colloid. Dynamic light scattering (DLS; Fig. 2E-H) was used to characterize the average flake size in the MXene colloids, indicating that the $Ti_3C_2T_x$ flakes were on average 280 nm, with flakes up to 1 µm in size; $Mo_2Ti_2C_3T_x$, $Nb_4C_3T_x$, and $Ta_4C_3T_x$ had average flake sizes of 370, 150, and 810 nm, respectively. Scanning electron microscopy (SEM; Fig. 2I-L) was used to confirm successful delamination of the MXene flakes. From the representative image, the flakes used in this study are confirmed to be single layers (about 1 nm in thickness), with sizes commensurate with DLS. They have O, OH and F on the surface, which affect their chemical properties and biological activity.

Fig. 3 – SARS-CoV-2 characterization

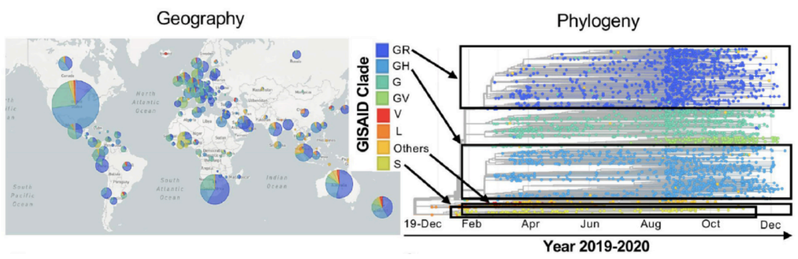

The Global Initiative on Sharing All Influenza Data (GISAID) platform classifies SARS-CoV-2 genomes into 8 clades and among which GR, GH and S clades have been identified in most of the countries, whereas the genomes from the clade designated as "other" is more specific to locations. In order to cover a wider range of SARS-CoV-2 genotypes present in most countries and carrying wild type or mutated viral proteins, we have selected 4 clades (GR, GH, S, and other) to test in this study.

Fig. 4 - Antiviral activity of $Ti_3C_2T_x$ on the infection of SARS-CoV-2

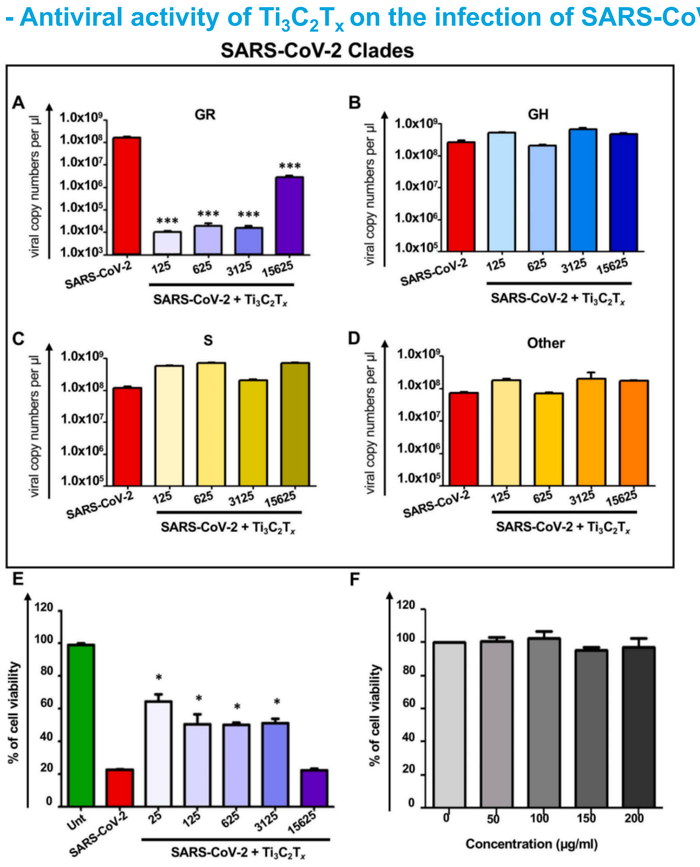

For evaluating MXene antiviral activity towards SARS-COV-2, we first selected $Ti_3C_2T_x$, the most widely used MXene type for biomedical applications. *In vitro* viral infection against SARS-CoV-2 was performed in the presence of the material in Vero E6 cells by using the four selected different viral clades (Fig. 4A-D). When cells were infected with SARS-CoV-2 in the presence of $Ti_3C_2T_x$, the viral copy number of GR clade was significantly reduced at every dilution tested, as compared to the cells treated with the virus alone. The viability of Vero E6 cells was significantly improved in the presence of the material, as compared to the cells treated with the virus alone (Fig. 4E). Also, no toxicity was observed when the cells were treated with only the nanomaterial (Fig. 4F).

Fig. 5 – Antiviral activity of other MXenes

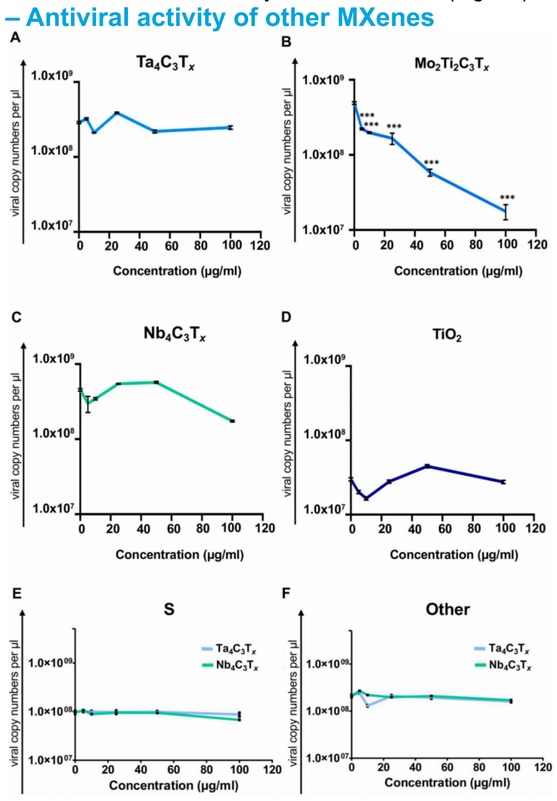

We selected viral particles from the clade GR to test other MXenes. No significant changes in viral copy number induced by $Ta_4C_3T_x$ and $Nb_4C_3T_x$ were observed, whereas $Mo_2Ti_2C_3T_x$ was able to induce more than 95% of viral inhibition. Titanium oxide (TiO_2) nanoparticles were used as a nanoparticle control group. Finally, we performed the antiviral activity assessment of non-Ti MXenes on the clades S and "other". Results showed that, similarly to the response obtained with the clade GR, there is no antiviral activity obtained with these materials.

Fig. 1 - Overview of the study design

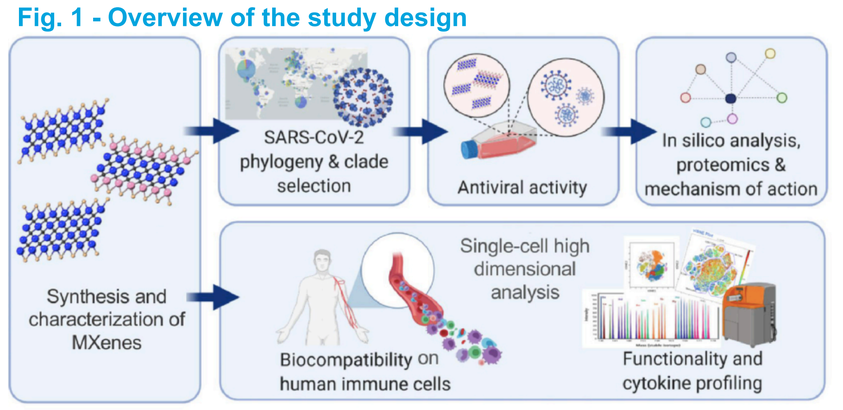

Fig. 6 – Proteomic analysis

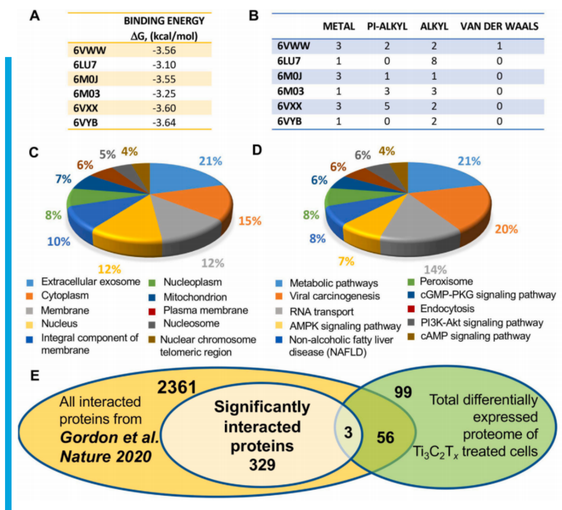

We carried out *in silico* molecular docking analysis to study the MXene targeted proteins and pathways during viral pathogenesis. The interactions of $Ti_3C_2T_x$ with different SARS-CoV-2 protein domains that have been shown to be the most important for SARS-CoV-2 infection were investigated. A proteomic analysis was performed to better explain the mechanism behind the viral inhibition. We performed LC-MS/MS analysis of Vero E6 cells following material exposure. The proteome analyses revealed a total of 158 differentially expressed proteins. Among them, upon material treatment, 90 proteins were up-regulated and 68 down-regulated.

Fig. 7 – MXene impact on immune cells at the single-cell level (CyTOF)

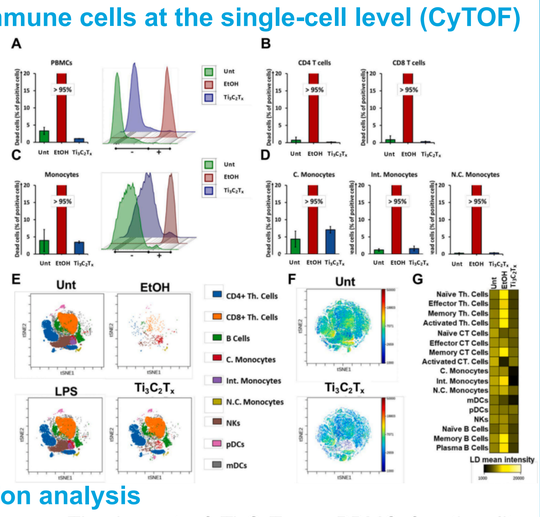

No significant loss of human peripheral blood mononuclear cell (PBMC) viability was observed by flow cytometry after treatment with $Ti_3C_2T_x$. Similar results were obtained also considering T cell and monocyte subpopulations. Moreover, the biocompatibility of the material was confirmed at the single-cell level on all immune cells subpopulations by single-cell mass cytometry (CyTOF).

Fig. 8 – Immune cell activation analysis

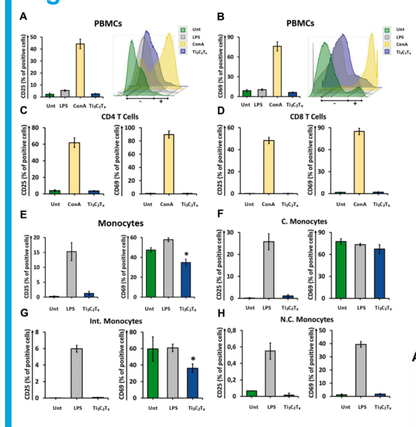

The impact of $Ti_3C_2T_x$ on PBMC functionality was evaluated by monitoring different activation parameters. No significant changes in either CD25 or CD69 expression in total PBMCs were observed. Moreover, no significant changes in the expression of CD25 and CD69 were observed in CD4 and CD8 T cells. Interestingly, $Ti_3C_2T_x$ induced a significant decrease of CD69 expression in total monocytes tracked down specifically to intermediate monocytes, leaving CD25 expression unchanged. These data suggest that MXenes may reduce intermediate monocytes pro-inflammatory activity.

Fig. 9 – Cytokine production

$Ti_3C_2T_x$ caused a downregulation of key mediator of SARS-CoV-2 acute respiratory distress syndrome, such as CXCL10, IL-2 and IL-4.

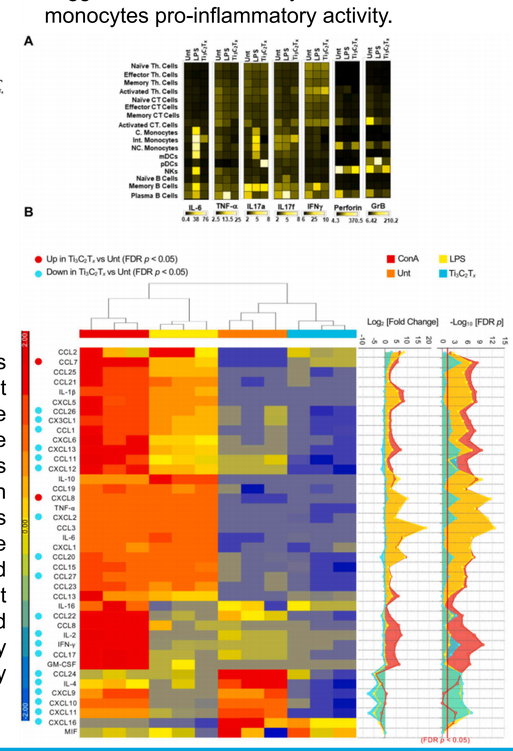

CONCLUSION

In conclusion, our study demonstrates the antiviral activity of MXenes against SARS-CoV-2. In addition, we established the high immune compatibility of MXenes as well as their anti-inflammatory effects on human immune cells. Our results serve as a guide to direct future studies to implement MXenes and other 2D nanomaterials in different biomedical technologies and nanomedicine tools, particularly against viral diseases, as well as any immune system-related syndromes.

CONTACT PERSON

laura.fusco@unipd.it;

luciagemma.delogu@unipd.it

REFERENCES

[1] M. Naguib, M. Kurtoglu, V. Presser, J. Lu, J. Niu, M. Heon, L. Hultman, Y. Gogotsi, M.W. Barsoum, Two-dimensional nanocrystals produced by exfoliation of Ti_3AlC_2, **Adv. Mater.** 23 (2011) 4248–4253.
[2] Y. Gogotsi, B. Anasori, The rise of MXenes, **ACS Nano** 13 (2019) 8491–8494.
[3] C. Weiss, M. Carriere, L. Fusco, I. Capua, J.A. Regla-Nava, M. Pasquali, J.A. Scott, F. Vitale, M.A. Unal, C. Mattevi, D. Bedognetti, A. Merkoçi, E. Tasciotti, A. Yilmazer, Y. Gogotsi, F. Stellacci, L.G. Delogu, Toward nanotechnology-enabled approaches against the COVID-19 pandemic, **ACS Nano** 14 (2020) 6383–6406.

chem2Dmat
AUGUST 31 - September 03, 2021 • ONLINE